

Supporting Information

Customised spatiotemporal temperature gradients created by a liquid metal enabled vortex generator

Jiu Yang Zhu, Peter Thurgood, Ngan Nguyen, Kamran Ghorbani, Khashayar Khoshmanesh †

School of Engineering, RMIT University, Melbourne, Victoria 3001, Australia

† Corresponding author: Khashayar.khoshmanesh@rmit.edu.au

Supporting Information 1: Mechanical clamp for holding the heat source

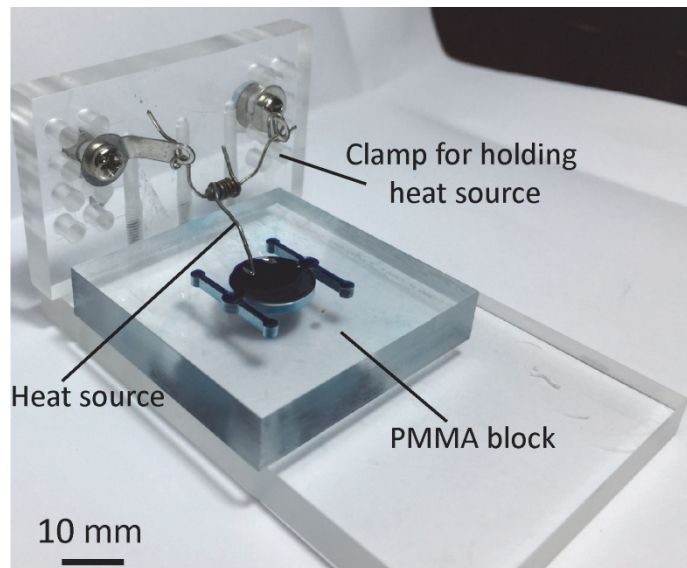


Figure S1. Mechanical clamp fabricated for holding the heat source inside the liquid chamber.

Supporting Information 2: Intrusion of liquid metal droplet into the liquid chamber

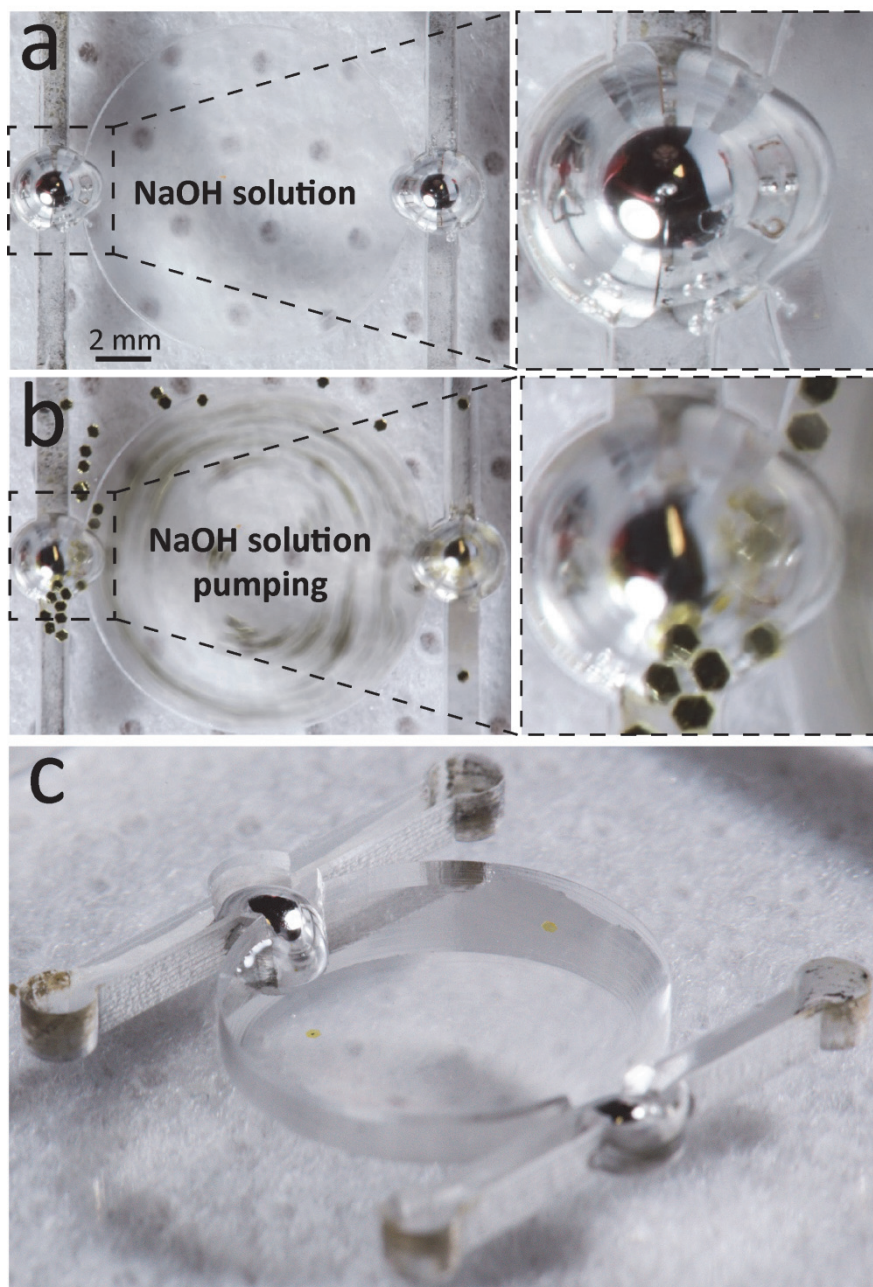


Figure S2. Intrusion of liquid metal droplet into the liquid chamber shown (a-b) before after applying voltage, and (c) in isometric view.

Supporting Information 3: Flow visualisation at the vicinity of liquid metal droplet

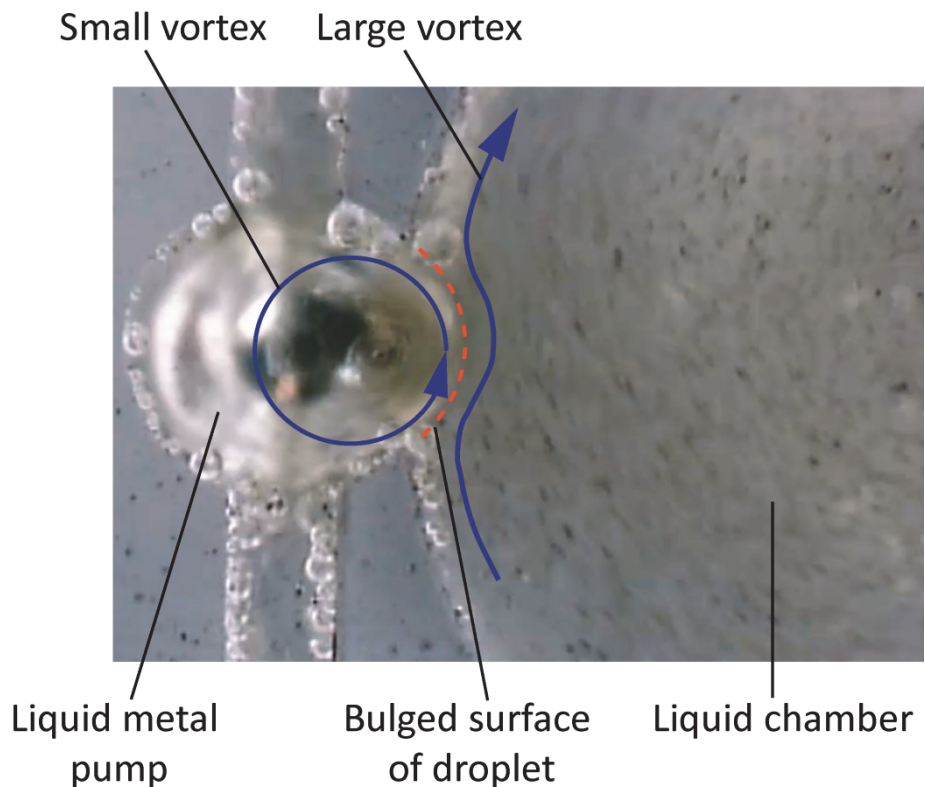


Figure S3. Flow visualisation using 100 μm colourant pigments added into the liquid chamber, showing the exsistence of a large vortex inside the liquid chamber and a small vortex above the liquid metal droplet, as presented in **Movie S3**.

Supporting Information 4: Numerical simulation of flow inside the liquid metal enabled vortex generator

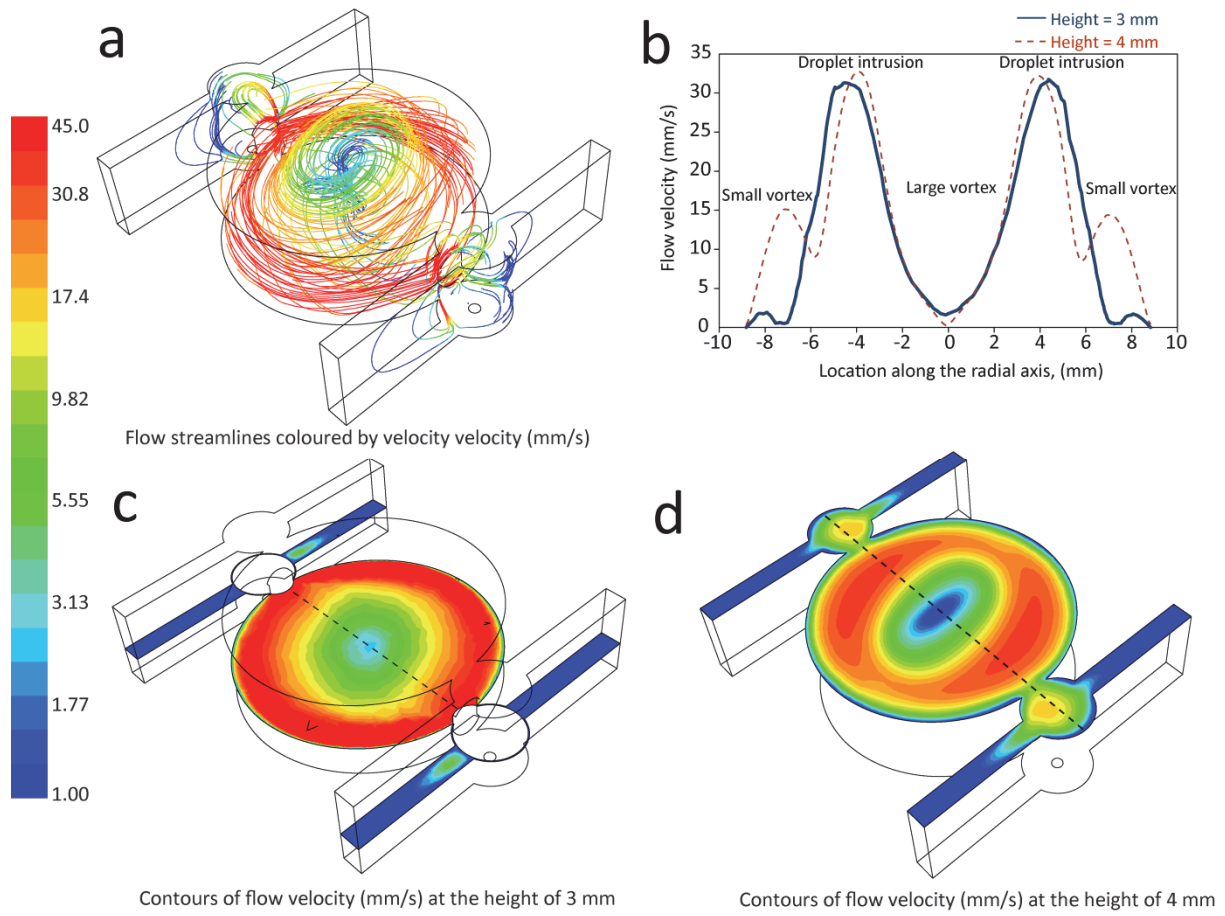


Figure S4. Analysis of flow patterns using computational fluid dynamics (CFD) method. The results are obtained by solving Navier-Stokes equations using ANSYS-Fluent software. The boundary conditions include a surface tension gradient at the surface of liquid metal droplet, zero shear stress at the top free surface of the chamber, and no-slip at the other surfaces: **(a)** The simulations clearly predict the formation of a large vortex inside the liquid chamber and two small vortices above the liquid metal droplets, **(b)** velocity profiles along the radial axis of liquid chamber at the heights of 3 and 4 mm, and **(c-d)** Velocity contours ant the hights of 3 and 4 mm.

Supporting Information 5: Liquid chambers with various orifice dimensions

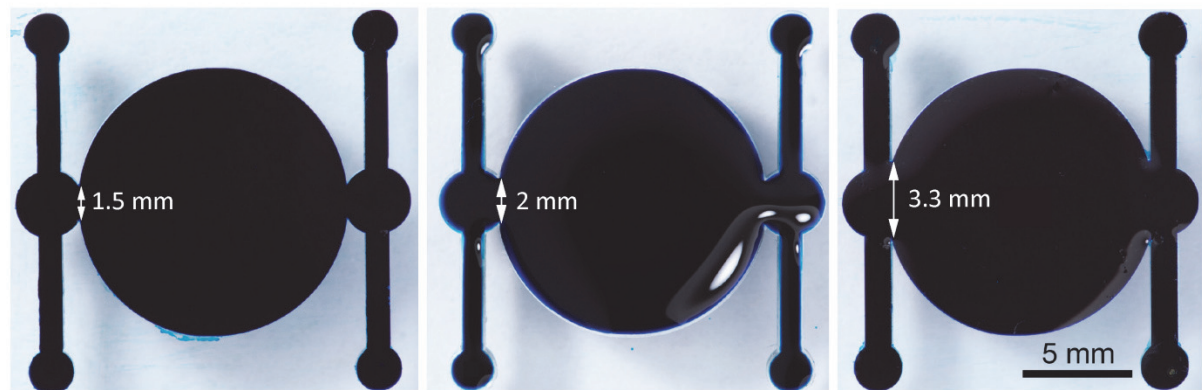


Figure S5. Liquid chambers with small, reference and large orifice widths.

Supporting Information 6: Liquid chambers with various diameters

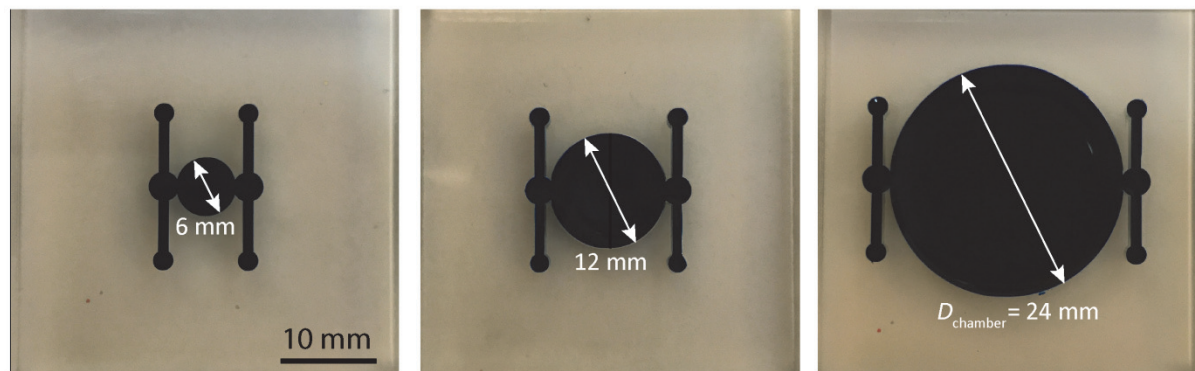


Figure S6. Liquid chambers with small, reference and large diameters.

Supporting Information 7: Raw temperature contours obtained after 5 minutes under different vortex modes

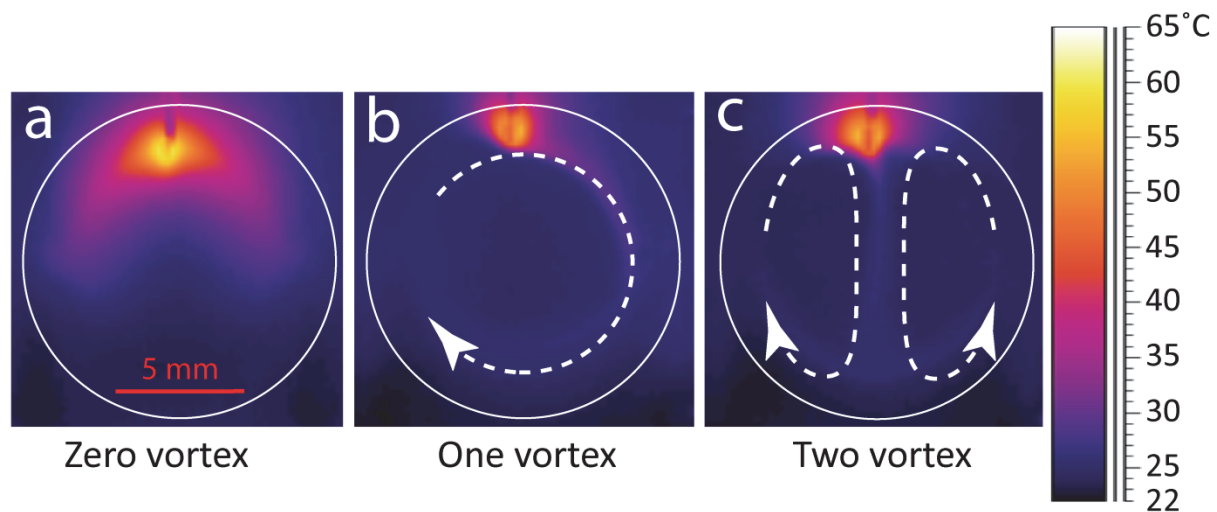


Figure S7: (a-c) Temperature distribution across the top free surface of the liquid chamber for zero, one and two vortex modes obtained by infrared camera when setting the temperature range from 22 to 65°C.

Supporting Information 8: Variations of vortex rotational speed and hot spot temperature against pump actuation frequency

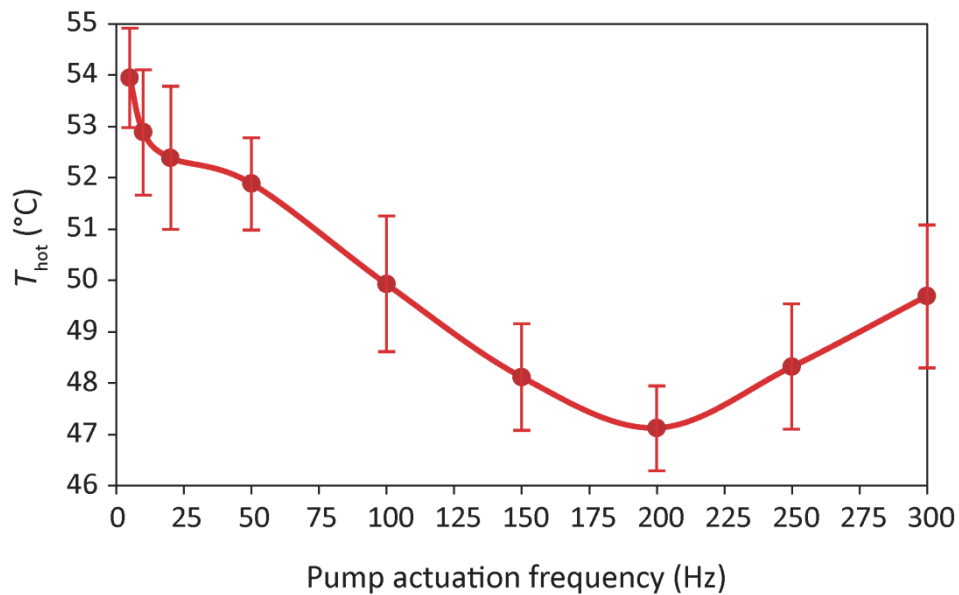


Figure S8: Maximum temperature against the frequency of square wave signal.

Supporting Information 9: Variations of temperature contours obtained in two vortex mode against pump actuation frequency

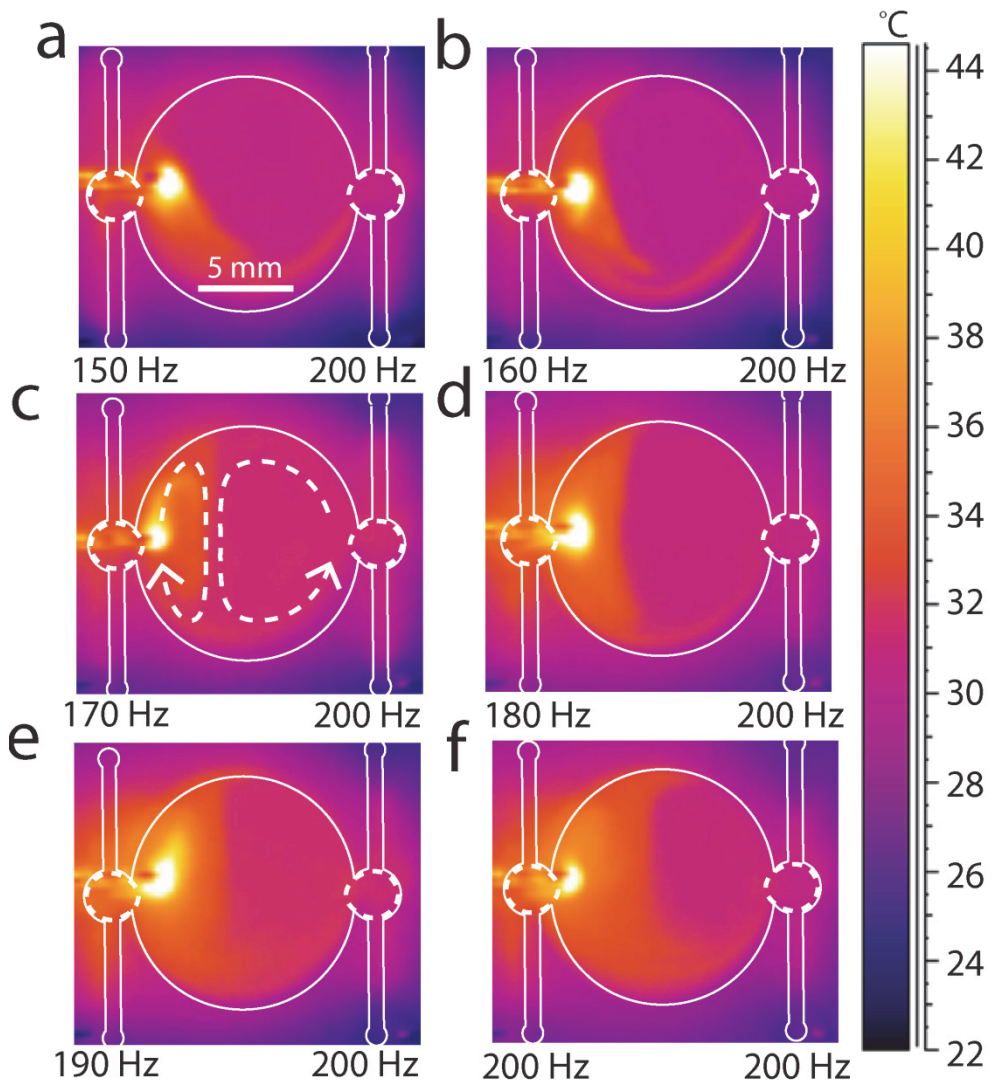


Figure S9: Temperature distribution across the top surface of liquid chamber when operating in two vortex mode while applying different frequencies to the liquid metal pumps.

Supporting Information 10: Raw temperature contours obtained after 1, 5 and 20 minutes under different vortex modes

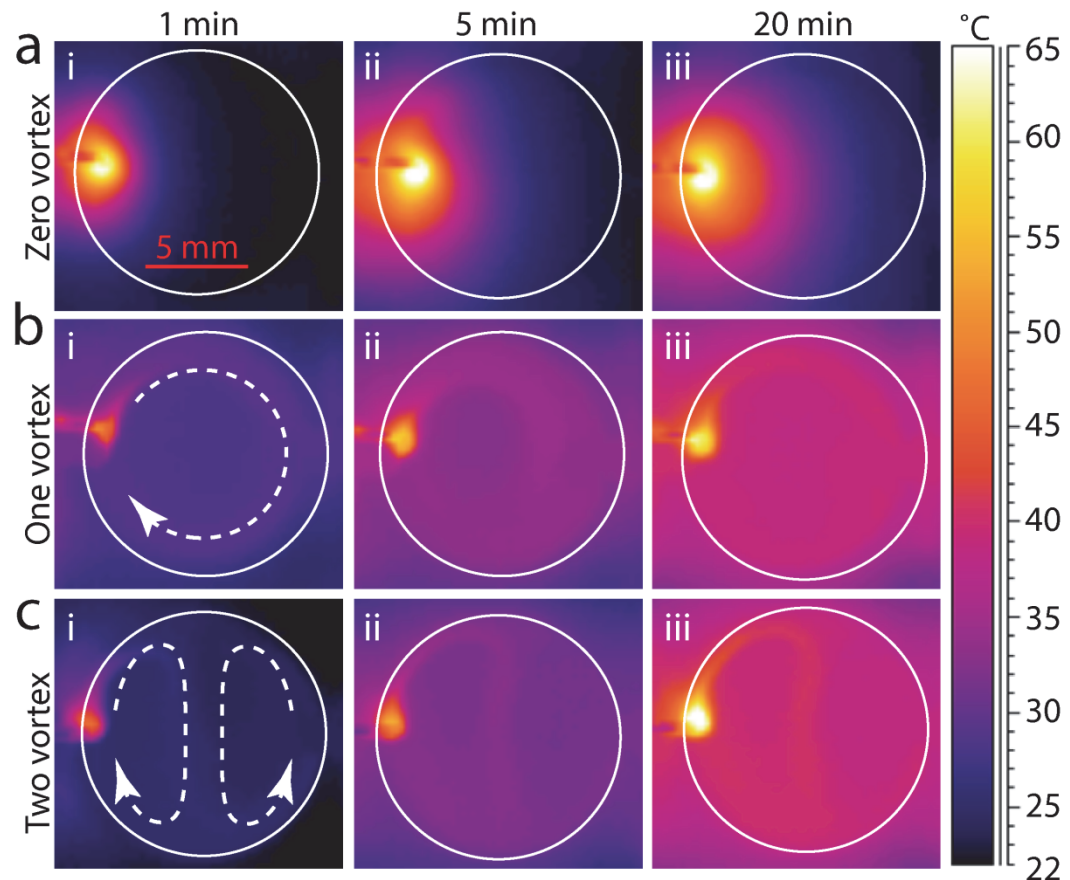


Figure S10: (a-c) Temperature distribution across the top free surface of the liquid chamber at 1, 5 and 20 minutes for zero, one and two vortex modes when setting the temperature range from 22 to 65°C.

Supporting Information 11: Customised spatiotemporal temperature gradients obtained by switching between two and zero vortex modes

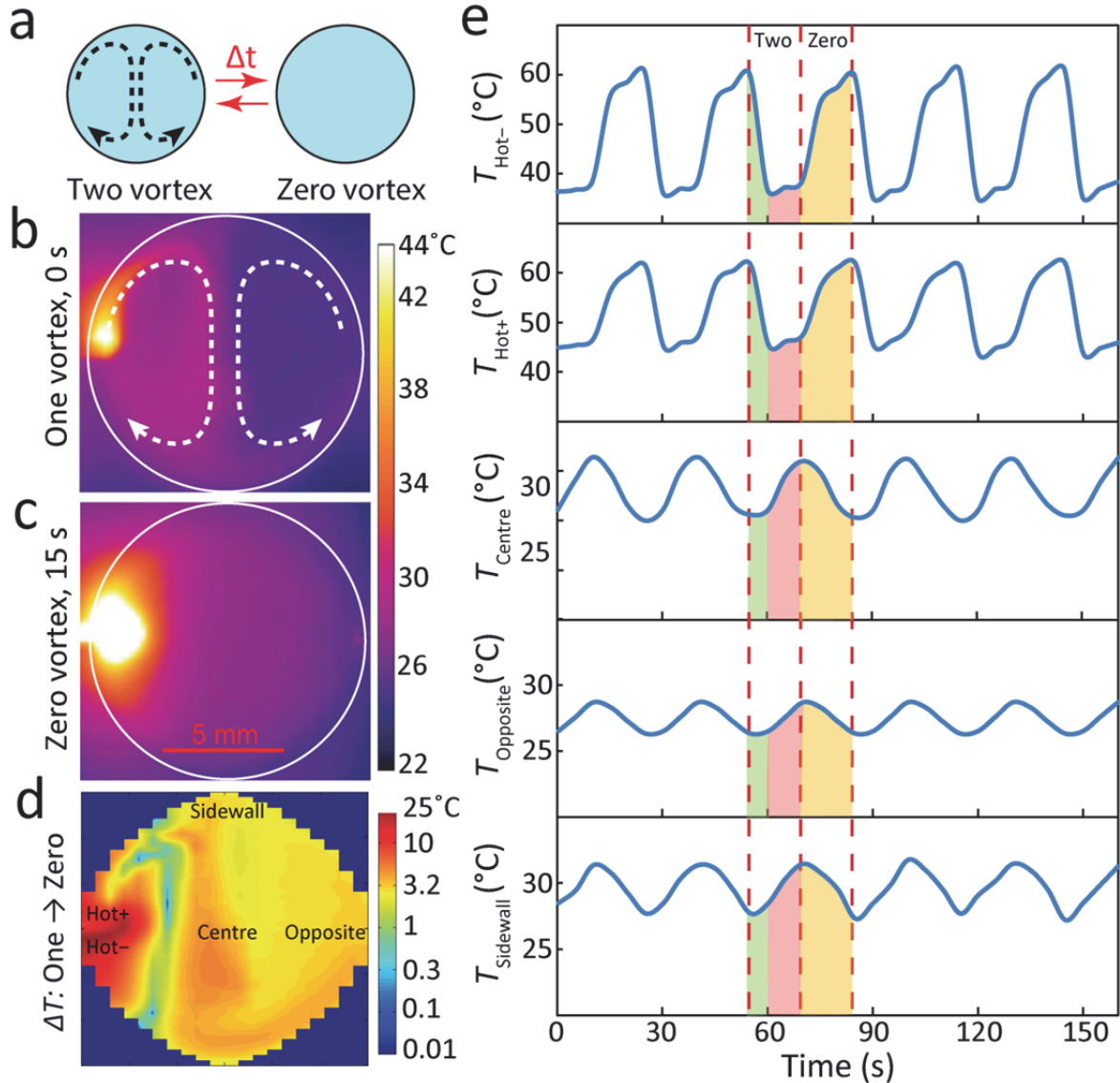


Figure S11: Creating customised spatiotemporal temperature gradients: (a) Consequential switching between two and zero vortex modes by setting the duration of each mode to 15 s, (b-c) Temperature distribution at the top free surface of the liquid chamber immediately after switching to one and zero vortex modes, (d) Amplitude of temperature oscillations across the liquid chamber when switching between one-zero vortex modes, calculated as: $\Delta T = |\langle T_{\text{one vortex}} \rangle_{t=0 \text{ s}} - \langle T_{\text{zero vortex}} \rangle_{t=15 \text{ s}}|$, (e) Temperature oscillations of the regions located at the hot spot upstream, hot spot downstream, vortex centre, sidewalls and opposite the hot spot.

Supporting Information 12: Customised spatiotemporal temperature gradients obtained by switching between one, two and zero vortex modes

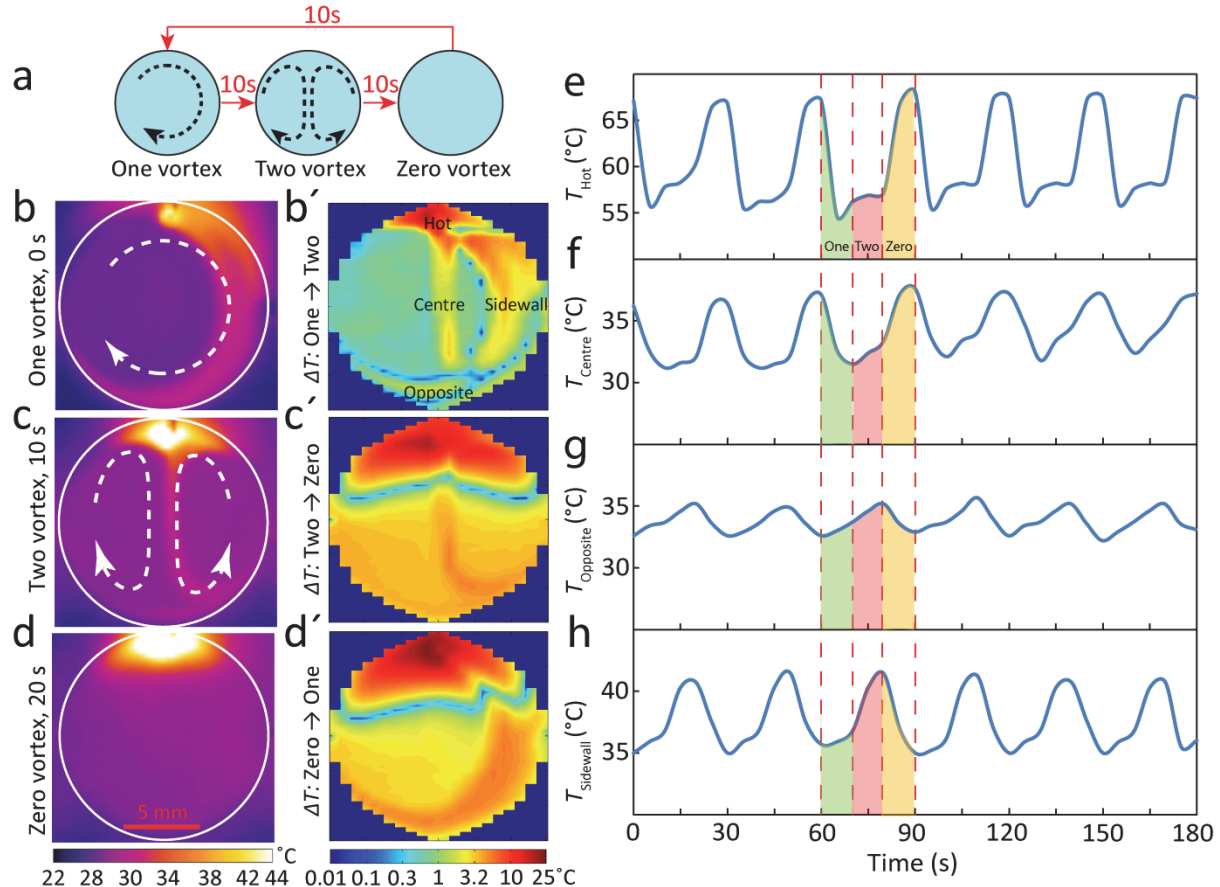


Figure S12i: Creating more complex spatiotemporal temperature gradients for the case of $\Delta t = 10$ s: **(a)** Consequential switching between one, two and zero vortex modes, **(b-d)** Temperature distribution at the top free surface of the liquid chamber immediately after switching to one, two and zero vortex modes, **(b'-d')** Amplitude of temperature oscillations across the liquid chamber for transient conditions obtained by switching from one \rightarrow two, two \rightarrow zero and zero \rightarrow one vortex modes when setting the duration of consequential vortex modes to $\Delta t = 10$ s, **(e-h)** Temperature oscillations obtained for the hot spot located at hot spot, vortex centre, sidewalls and opposite to hot spot.

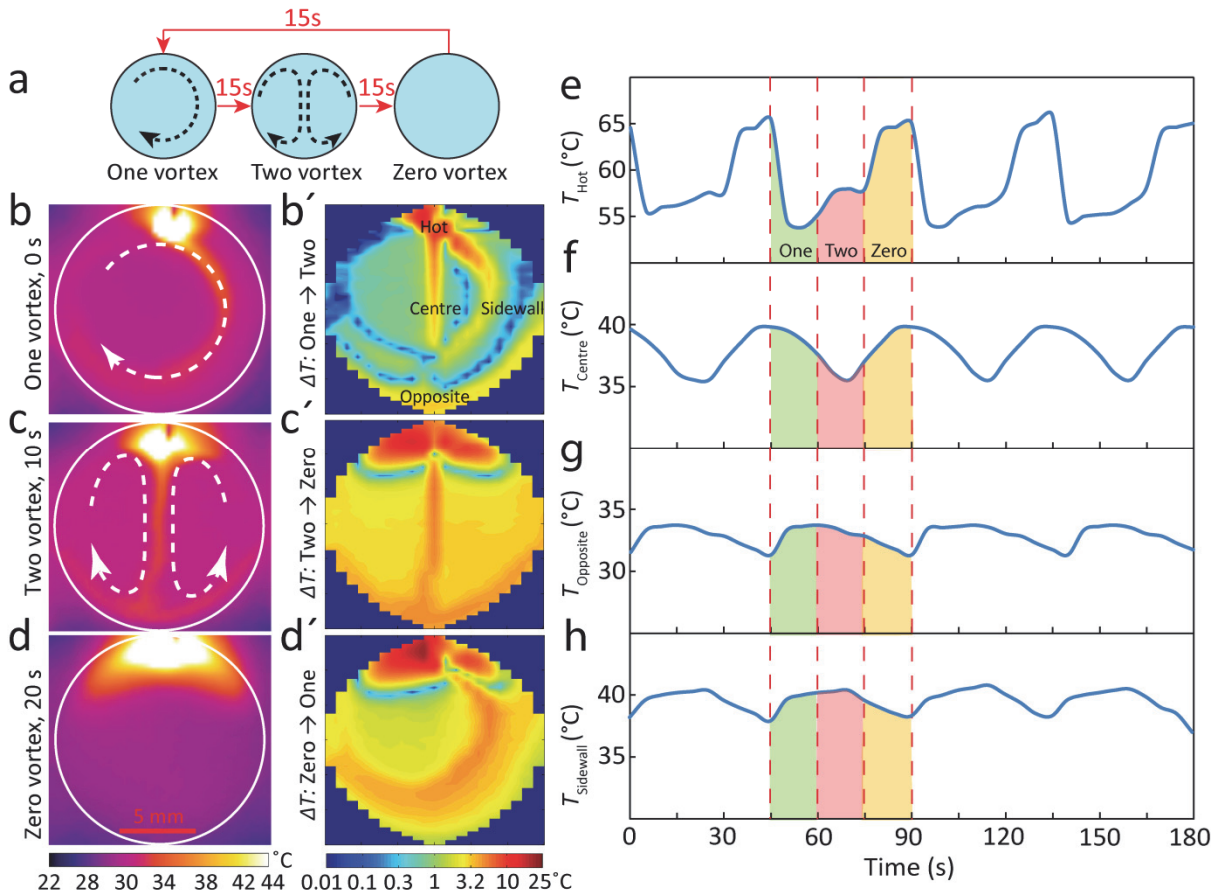


Figure S12ii: Creating more complex spatiotemporal temperature gradients for the case of $\Delta t = 15$ s: **(a)** Consequential switching between one, two and zero vortex modes, **(b-d)** Temperature distribution at the top free surface of the liquid chamber immediately after switching to one, two and zero vortex modes, **(b'-d')** Amplitude of temperature oscillations across the liquid chamber for transient conditions obtained by switching from one \rightarrow two, two \rightarrow zero and zero \rightarrow one vortex modes when setting the duration of consequential vortex modes to $\Delta t = 15$ s, **(e-h)** Temperature oscillations obtained for the hot spot located at hot spot, vortex centre, sidewalls and opposite to the hot spot.

Supporting Information 13: Various vortex patterns by implementing more liquid metal pumps

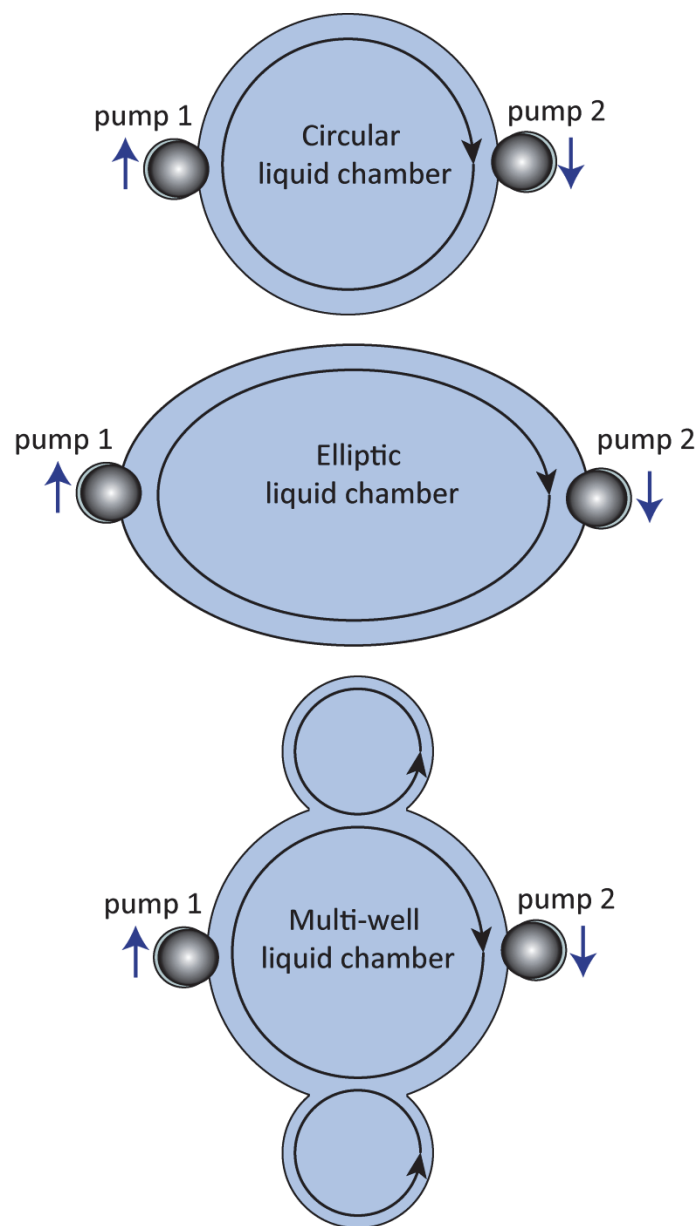


Figure S13i: Various vortex patterns by changing the geometry of the liquid chamber

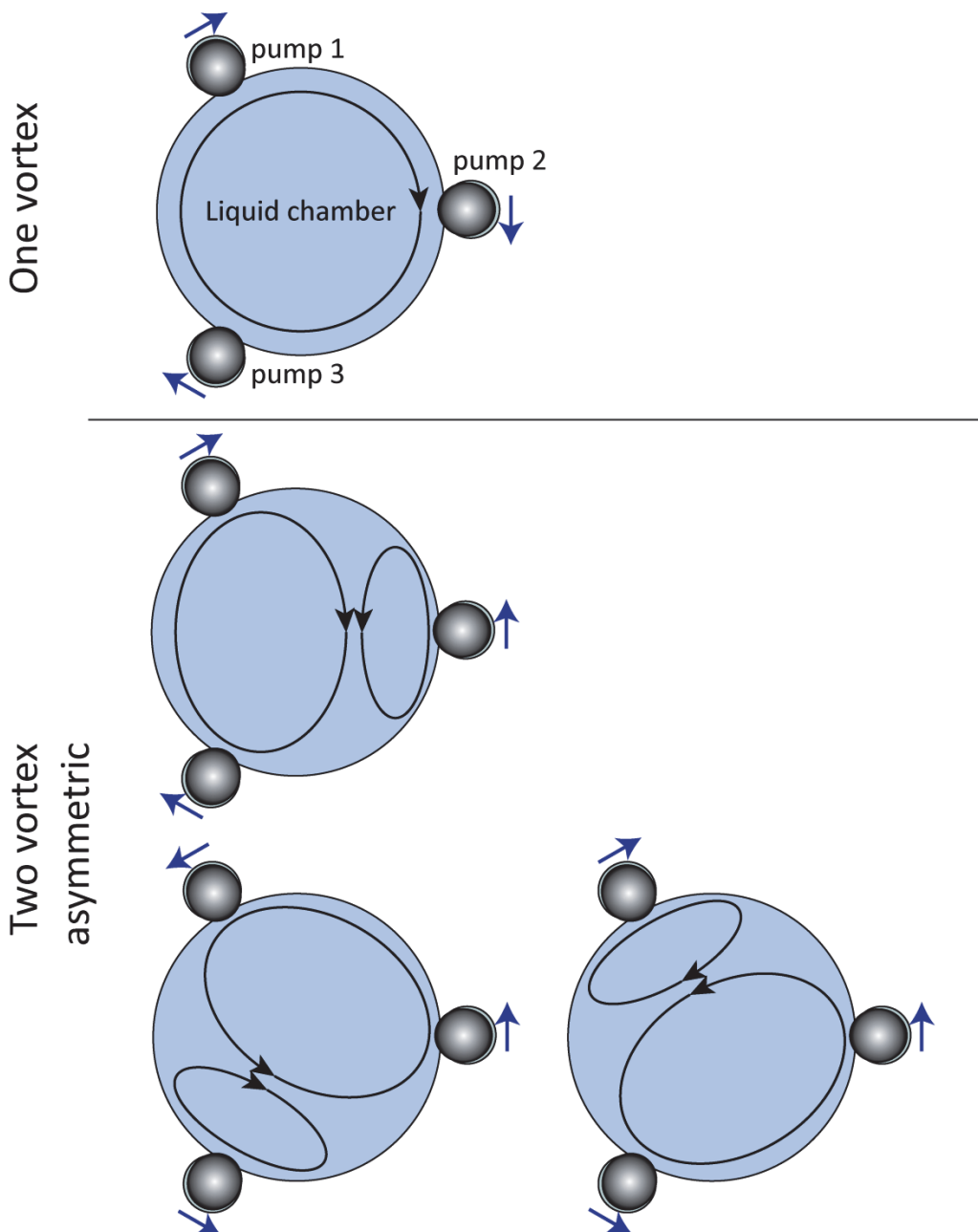


Figure S13ii: Various vortex patterns by implementing three liquid metal pumps

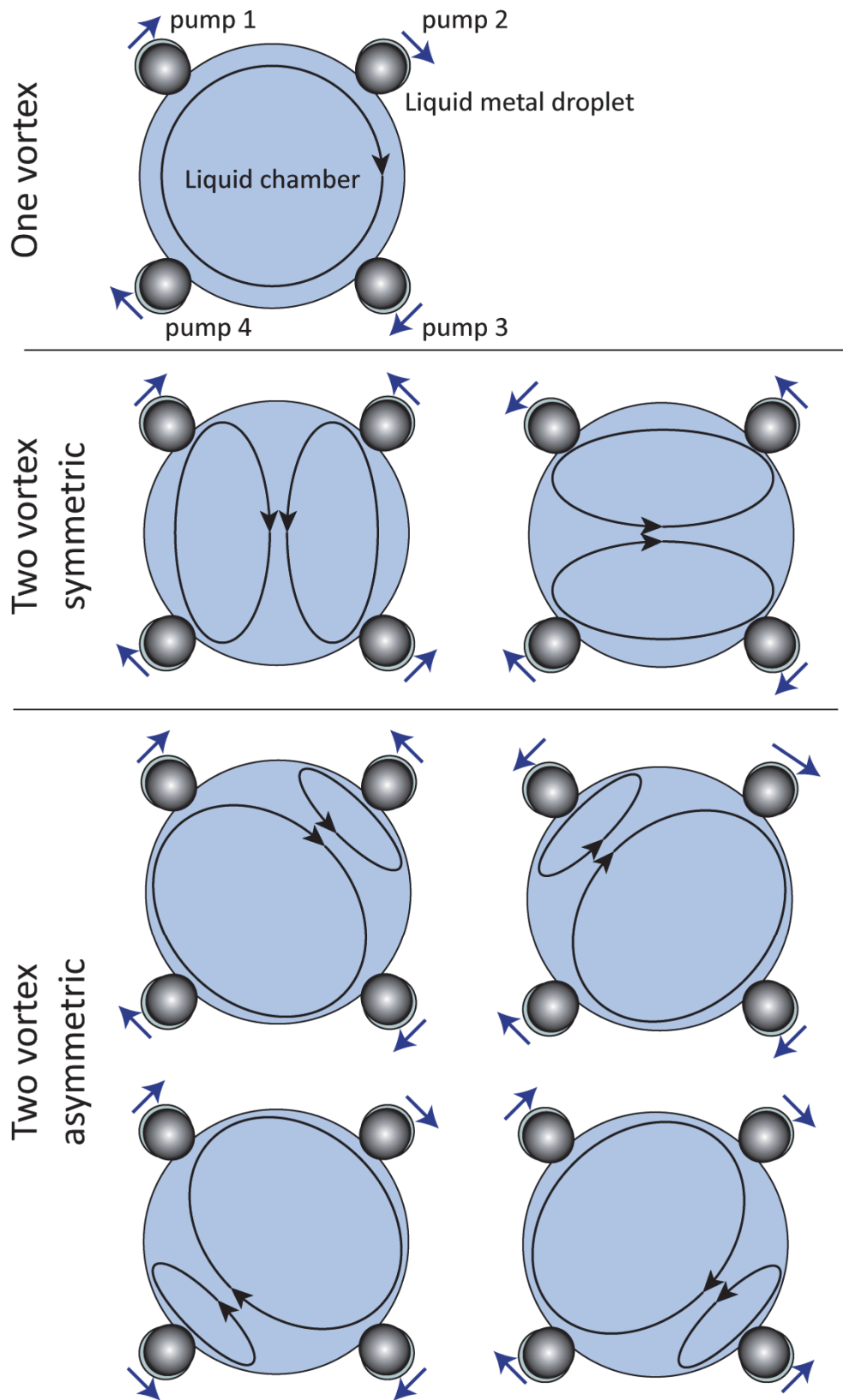


Figure S13iiii: Various vortex patterns by implementing four liquid metal pumps